
Fully convolutional Siamese neural networks for buildings damage assessment from satellite images

Eugene Khvedchenya
Computer vision research engineer
Piñata Farms
Odessa, Ukraine
ekhvedchenya@gmail.com

Tatiana Gabruseva
Independent researcher
Cork, Ireland
tatigabru@gmail.com

Abstract

Damage assessment after natural disasters is needed to distribute aid and forces to recovery from damage dealt optimally. This process involves acquiring satellite imagery for the region of interest, localization of buildings, and classification of the amount of damage caused by nature or urban factors to buildings. In case of natural disasters, this means processing many square kilometers of the area to judge whether a particular building had suffered from the damaging factors.

In this work, we develop a computational approach for an automated comparison of the same region's satellite images before and after the disaster, and classify different levels of damage in buildings. Our solution is based on Siamese neural networks with encoder-decoder architecture. We include an extensive ablation study and compare different encoders, decoders, loss functions, augmentations, and several methods to combine two images. The solution achieved one of the best results in the Computer Vision for Building Damage Assessment competition.

1 Application Context

Natural disasters require quick and accurate situational information for an effective response. Before responders can act in the affected area, they need to know the locations and severity of damage as soon as possible. Damage assessment involves acquiring satellite imagery for the region of interest, localization of buildings, and classification of damage degree caused to the buildings. High-resolution imagery is required to see the details of specific damage conditions. Current response strategies require in-person damage assessments within 24-48 hours of a disaster. The large areas affected combined with the vast numbers of pixels representing those areas make it laborious for analysts to search and evaluate damages in a disaster area. Therefore, an automated damage assessment of buildings after natural disasters would greatly help distribute humanitarian forces optimally. Here, we present the solution of the xView2 Computer Vision for Building Damage Assessment Challenge, hosted at <https://www.xview2.org/>. Our algorithm locates and compares buildings on two corresponding images before and after the disaster and classifies their damage level.

Deep learning approaches are widely used for the automatic extraction of information from satellite images Solovyev [2020], Iglovikov et al. [2018], Buslaev et al. [2018], Seferbekov et al. [2018]. Siamese networks have shown great success in finding similar/dissimilar image pairs Dey et al. [2017], Chicco [2020]. Using a shared backbone to extract embeddings from two images, they can effectively learn discriminative features in the fully-connected layer. Siamese networks with encoder-decoder architecture were proposed for the change detection in Caye Daudt R. and A. [2018]. Our solution is based on an end-to-end architecture that allows simultaneously locate objects on a pair of images and compare the difference between them. We describe practical techniques that help to improve the model's performance. We study various encoders, decoders, loss functions, augmentations, and

different methods to combine input images. The source code is publicly available at Khvedchenya [2020] under the MIT license.

2 Problem statement

In the challenge, given a pair of images before ("pre") and after ("post") a natural disaster, solutions should output a semantic mask that corresponds to the "pre" image and classifies each pixel in one of the classes: 0 - "no building", 1 - "building, no damage", 2 - "building, minor damage", 3 - "building, major damage", and 4 - "building, destroyed". The details on the four-level damage scale are given in Gupta et al. [2019].

A target objective in the challenge was a weighted sum of F_1 scores for building localization, F_{1loc} , and damage classification, F_{1class} tasks, defined as follows:

$$Score = 0.3 * F_{1loc} + 0.7 * F_{1class}. \quad (1)$$

3 Dataset

The dataset xBD Gupta et al. [2019] contained 18336 high-resolution satellite images, covering a diverse set of disasters with over 850,000 buildings across over 45,000 km² of imagery. The dataset contained pairs of images of the same region before ("pre") and after ("post") a natural disaster and included data from 15 countries and 6 types of disasters. All images had a resolution of 1024 x 1024 pixels. The dataset was highly unbalanced in terms of damage degree, area of imagery, and polygons per disaster event. The distribution of damage classes was highly skewed towards "no damage" Gupta et al. [2019].

The images were manually annotated with polygons. Each polygon represented a building/structure and was labeled with a degree of damage that occurred to it during the disaster, scaled from 1 to 4. The main objective of the challenge was to build a solution capable of processing a pair of satellite images of the same region before and after a disaster and assessing buildings' level of damage. Figure 1 shows an example of the satellite images and the corresponding ground truth mask.



Figure 1: Examples of the satellite imagery collected before (a) and after (b) the disaster and the corresponding ground truth mask (c). The color of the buildings represents the damage degree, with totally destroyed buildings in red and undestroyed in blue.

4 Methodology

The goal in the given task is two-fold: a) detecting buildings in the "pre-disaster" image, b) evaluate each building's damage concerning its counterpart in the "post-disaster" image. One can solve this problem by performing semantic segmentation using pairs of input images.

For training, we generated masks with 1024 x 1024 resolution that contained 5 classes with values: 0 - "no building", 1 - "building, no damage", 2 - "building, minor damage", 3 - "building, major damage", and 4 - "building, destroyed". The models were trained to predict a multi-class segmentation mask with five classes. All models were trained on crops of 512 x 512 px size and validated on

full-resolution images of 1024 x 1024 px. For validation, the training set was split into five folds using multi-label stratification based on the amount and severity of damaged buildings. Five-folds cross-validation was used to find optimal model architectures and tune hyperparameters.

4.1 Model architecture

There is a wide range of deep learning architectures for semantic segmentation Lin et al. [2016], Ronneberger et al. [2015], Zhao et al. [2017]. Most of them follow the encoder-decoder principle. The encoder extracts representative feature maps of different spatial dimensions, and the decoder reconstructs a full-resolution semantic mask.

Unlike typical image segmentation tasks, this problem needs two images to produce predictions. There are several ways to input two images into the model. The most straightforward approach is to concatenate "pre-disaster" and "post-disaster" images from the pair into a single tensor with six channels and use it as an input. Another approach is to train the same backbone using both input images simultaneously. Siamese networks have shown great success in finding similar/dissimilar image pairs Dey et al. [2017], Chicco [2020], Caye Daudt R. and A. [2018]. Using a shared backbone to extract embeddings from two images, they can effectively learn discriminative features in the fully connected layer.

The Siamese network architecture for this task was designed as follows:

- Using a shared encoder extract feature maps of strides [2, 4, 8, 16, 32] for "pre-disaster" and "post-disaster" images.
- Concatenate/subtract feature maps for each stride together along channels dimension.
- Feed concatenated feature maps to the decoder (we studied Unet and FPN decoders).

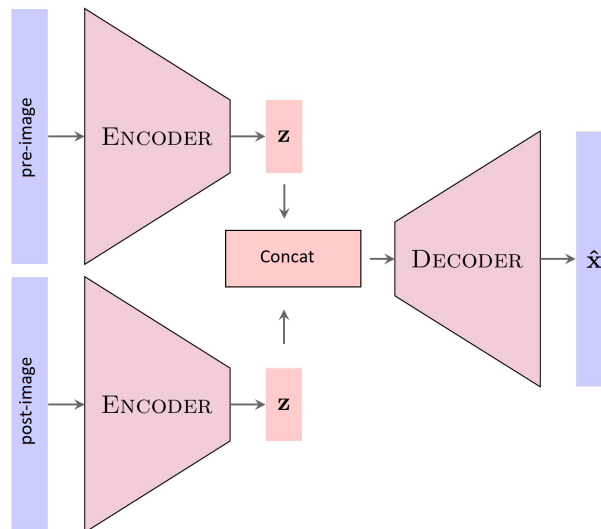


Figure 2: Schematic architecture of the hybrid Siamese encoder-decoder architecture.

This hybrid Siamese architecture is shown schematically in Figure 2.

4.2 Images pre-processing and augmentations

The original images were cropped and resized to 512 x 512 px resolution for training. The validation was performed on the full-resolution images, 1024 x 1024 px. For augmenting images, we used an open-source library Albumentations Buslaev et al. [2020]. The following image augmentations were applied during training phase:

- **Spatial transformation, applied to only "post" images:** random rotation up to 3 degree, random shift by (-10,+10) pixels, random scale in the range -2% .. +2%

- **Spatial transformation, applied to both "pre" and "post" images:** crop 512x512 patches for same region, random scale varying from 80% to 120%, horizontal flip, rotation by 90 degrees, transpose, random grid shuffle, mask dropout
- **Color augmentations, applied independently to "pre" and "post" images:** random brightness, contrast and gamma change, changes in HSV or RGB colorspace

Heavy spatial augmentations were applied in the same manner to both "pre" and "post" images to ensure consistency in their crops. Color augmentations, on the other side, were applied independently.

5 Results: Ablation study

5.1 Combining input images: basic model architecture

We compare Siamese networks to the classical segmentation approach, based on concatenation of "pre-disaster" and "post-disaster" into a 6-channel tensor and sending it through an encoder-decoder model. The results are shown in Table 2 for various ResNet He et al. [2015] encoders, Unet decoder, and identical training parameters. We show localization, classification and weighted F_1 scores obtained for different models' architectures on a validation set. The Siamese architectures outperform by far the classical encoder-decoder architecture, especially for the damage classification task. The concatenation of features in the Siamese network outperformed subtraction for most of the encoders, although the difference is relatively small.

Table 1: Localization, damage and weighted F_1 scores obtained for different models' architectures on a validation set

Approach	Encoder/Decoder	F_{1loc}	F_{1class}	F_1
concatenation	ResNet18/Unet	0.8649	0.6784	0.7344
concatenation	ResNet34/Unet	0.8475	0.6098	0.7211
concatenation	ResNet50/Unet	0.8707	0.6833	0.7395
Siamese, concat	ResNet18/Unet	0.8638	0.6831	0.7373
Siamese, concat	ResNet34/Unet	0.8720	0.7249	0.7690
Siamese, concat	ResNet50/Unet	0.8726	0.7218	0.7670
Siamese, subtract	ResNet18/Unet	0.8618	0.7255	0.7664
Siamese, subtract	ResNet34/Unet	0.8616	0.7166	0.7601
Siamese, subtract	ResNet50/Unet	0.8664	0.7188	0.7631

5.2 Effect of augmentations and weighted entropy loss

We ran an ablation study using a Siamese architecture with ResNet-34 encoder and Unet decoder to measure the influence of image augmentations on the model performance. The results are presented in Table 2. Using both spatial and color augmentations helped improve the model accuracy, especially for the damage classification task, compared to the setting without transforms or for color transforms only. Using strong transformations did not bring any further improvements in the model performance. A default choice for loss function for semantic segmentation is cross-entropy (CE) loss. In the damage detection task, a critical problem is overcoming classes imbalance, as the majority of buildings are not affected or affected less severely. To address this challenge, we propose a weighted CE loss. We assigned weights of 1.0 to the most common "not building" and "no damage" classes and weights of 3.0 to less popular "minor", "major" and "destroyed" classes. Such weighting of under-represented classes helped to increase F_1 score on those classes. We found that a CE loss with class weights worked better for this challenge as it provides compensation for the class imbalance.

5.3 Different encoders and decoders

We used feature extractors pre-trained on ImageNet dataset Cadene [2020]. A number of different encoder architectures has been studied: ResNet-18, -34, -50, -101 He et al. [2015], DenseNet-169, -201 Huang et al. [2017], SE-ResNext-50 Hu et al. [2018], Inception-v4 Szegedy et al. [2016], and

Table 2: Localization and damage classification F_1 scores, and weighted F_1 score achieved for Siamese ResNet-34/Unet architecture for different losses and augmentations

Model	Loss	Augmentations	F_{1loc}	F_{1class}	Score
ResNet34/Unet	CE	Medium	0.8765	0.7096	0.7597
ResNet34/Unet	Weighted CE	Medium	0.8720	0.7249	0.7690
ResNet34/Unet	Weighted CE	None	0.8704	0.7068	0.7559
ResNet34/Unet	Weighted CE	Color only	0.8716	0.7061	0.7558
ResNet34/Unet	Weighted CE	Hard	0.8712	0.7246	0.7686

EfficientNet Tan and Le [2019]. Table 3 shows validation scores for various encoders and decoders architectures. The lightest encoders, like ResNet-18, produced significantly lower results for both building localization and damage classification, showing underfitting for this problem. The models with heavier encoders generally achieved better results for the same decoder type. The SE-ResNext-50 encoder architecture demonstrated the best performance on this dataset both for localization and classification, achieving a weighted F_1 score of 0.78 for a single fold model. DenseNets also gave close results.

Table 3: Scores for buildings localization, F_{1loc} , damage classification, F_{1class} , and weighted F_1 score, achieved with various encoder-decoder models’ architectures on a validation set.

Encoder	Decoder	F_{1loc}	F_{1class}	Score
ResNet18	Unet	0.8638	0.6831	0.7373
ResNet34	Unet	0.8720	0.7249	0.7690
ResNet50	Unet	0.8726	0.7218	0.7670
ResNet101	Unet	0.8738	0.7225	0.7679
DenseNet169	Unet	0.8740	0.7293	0.7727
Se-ResNext50	Unet	0.8797	0.7338	0.7776
ResNet101	FPN	0.8710	0.7143	0.7613
Inception-v4	FPN	0.8332	0.7199	0.7539
Efficient-b4	FPN	0.8605	0.7213	0.7631

The Unet decoder produced slightly better results than FPN for the same encoders. The difference in performance for the Unet or FPN was relatively small. The choice on the pre-trained encoder had higher influence on the overall model performance, especially, for the classification task.

6 Conclusions

In this work, we develop a computational approach for automated building localization and their damage assessment from a pair of satellite images. We consider several methods to combine the input images or their feature maps. The Siamese architecture outperformed by far the classical approach with concatenated input images and achieved one of the best results in the Computer Vision for Building Damage Assessment competition. Concatenating feature maps before the decoder part performed slightly better than their subtraction. We tested different decoders and encoders and introduced a number improvements were implemented that helped to increase the performance of the model. The extensive ablation study has shown the effect of these modifications on the model’s performance. The source code is publicly available at Khvedchenya [2020].

References

- Alexander Buslaev, Selim Seferbekov, Vladimir Iglovikov, and Alexey Shvets. Fully convolutional network for automatic road extraction from satellite imagery. In *Proceedings of the IEEE Conference on Computer Vision and Pattern Recognition (CVPR) Workshops*, June 2018.
- Alexander Buslaev, Vladimir Iglovikov, Eugene Khvedchenya, Alex Parinov, Mikhail Druzhinin, and Alexandr Kalinin. Albumentations: Fast and flexible image augmentations. *Information*, 11(2), 2020. ISSN 2078-2489. doi: 10.3390/info11020125. URL <https://www.mdpi.com/2078-2489/11/2/125>.

- Remi Cadene. Pytorch pretrained models. <https://github.com/Cadene/pretrained-models.pytorch>, 2020. URL <https://github.com/Cadene/pretrained-models.pytorch>.
- Le Saux B, Caye Daudt R. and Boulch A. Fully convolutional siamese networks for change detection. In *Proceedings of the IEEE International Conference on Image Processing (ICIP)*, pages 4063–4067, 2018. doi: 10.1109/ICIP.2018.8451652.
- Davide Chicco. Siamese neural networks: An overview. In *Methods in Molecular Biology*, pages 73–94. Springer US, aug 2020. doi: 10.1007/978-1-0716-0826-5_3.
- Sounak Dey, Anjan Dutta, J. Ignacio Toledo, Suman K. Ghosh, Josep Lladós, and Umapada Pal. Signet: Convolutional siamese network for writer independent offline signature verification. *ArXiv*, 2017.
- Ritwik Gupta, B. Goodman, Nirav Patel, Richard Hosfelt, Sandra Sajeev, E. Heim, J. Doshi, K. Lucas, H. Choset, and M. Gaston. Creating xbd: A dataset for assessing building damage from satellite imagery. *ArXiv*, abs/1911.09296, 2019.
- Kaiming He, Xiangyu Zhang, Shaoqing Ren, and Jian Sun. Deep residual learning for image recognition, 2015. URL <https://arxiv.org/abs/1512.03385>.
- Jie Hu, Li Shen, and Gang Sun. Squeeze-and-excitation networks. In *The IEEE Conference on Computer Vision and Pattern Recognition (CVPR)*, June 2018.
- Gao Huang, Zhuang Liu, Laurens Van Der Maaten, and Kilian Q. Weinberger. Densely connected convolutional networks. In *2017 IEEE Conference on Computer Vision and Pattern Recognition (CVPR)*. IEEE, jul 2017. doi: 10.1109/cvpr.2017.243.
- Vladimir Iglovikov, Selim Seferbekov, Alexander Buslaev, and Alexey Shvets. Terausnetv2: Fully convolutional network for instance segmentation. In *Proceedings of the IEEE Conference on Computer Vision and Pattern Recognition (CVPR) Workshops*, June 2018.
- Eugene Khvedchenya. Pytorch toolbelt library. <https://github.com/BloodAxe/pytorch-toolbelt>, 2019. URL <https://github.com/BloodAxe/pytorch-toolbelt>.
- Eugene Khvedchenya. Bloodaxe: xview2-solution. <https://github.com/BloodAxe/xView2-Solution>, 2020.
- Sergey Kolesnikov. Accelerated deep learning randd. <https://github.com/catalyst-team/catalyst>, 2018.
- Tsung-Yi Lin, Piotr Dollár, Ross Girshick, Kaiming He, Bharath Hariharan, and Serge Belongie. Feature pyramid networks for object detection. *arXiv*, 2016. URL <http://arxiv.org/pdf/1612.03144v2:PDF>.
- Liyuan Liu, Haoming Jiang, Pengcheng He, Weizhu Chen, Xiaodong Liu, Jianfeng Gao, and Jiawei Han. On the variance of the adaptive learning rate and beyond. In *Proceedings of the Eighth International Conference on Learning Representations (ICLR 2020)*, April 2020.
- Adam Paszke, Sam Gross, Francisco Massa, Adam Lerer, James Bradbury, Gregory Chanan, Trevor Killeen, Zeming Lin, Natalia Gimelshein, Luca Antiga, Alban Desmaison, Andreas Kopf, Edward Yang, Zachary DeVito, Martin Raison, Alykhan Tejani, Sasank Chilamkurthy, Benoit Steiner, Lu Fang, Junjie Bai, and Soumith Chintala. Pytorch: An imperative style, high-performance deep learning library. In H. Wallach, H. Larochelle, A. Beygelzimer, F. d'Alché-Buc, E. Fox, and R. Garnett, editors, *Advances in Neural Information Processing Systems 32*, pages 8024–8035. Curran Associates, Inc., 2019.
- O. Ronneberger, P. Fischer, and T. Brox. U-net: Convolutional networks for biomedical image segmentation. *ArXiv*, abs/1505.04597, 2015.
- Selim Seferbekov, Vladimir Iglovikov, Alexander Buslaev, and Alexey Shvets. Feature pyramid network for multi-class land segmentation. In *Proceedings of the IEEE Conference on Computer Vision and Pattern Recognition (CVPR) Workshops*, June 2018.
- R. Solov'yev. Roof material classification from aerial imagery. *ArXiv*, abs/2004.11482, 2020.
- Christian Szegedy, Sergey Ioffe, Vincent Vanhoucke, and Alex Alemi. Inception-v4, inception-resnet and the impact of residual connections on learning, 2016. URL <https://arxiv.org/abs/1602.07261>.
- Mingxing Tan and Quoc Le. Efficientnet: Rethinking model scaling for convolutional neural networks. In Kamalika Chaudhuri and Ruslan Salakhutdinov, editors, *Proceedings of the 36th International Conference on Machine Learning*, volume 97 of *Proceedings of Machine Learning Research*, pages 6105–6114. PMLR, 09–15 Jun 2019. URL <http://proceedings.mlr.press/v97/tan19a.html>.

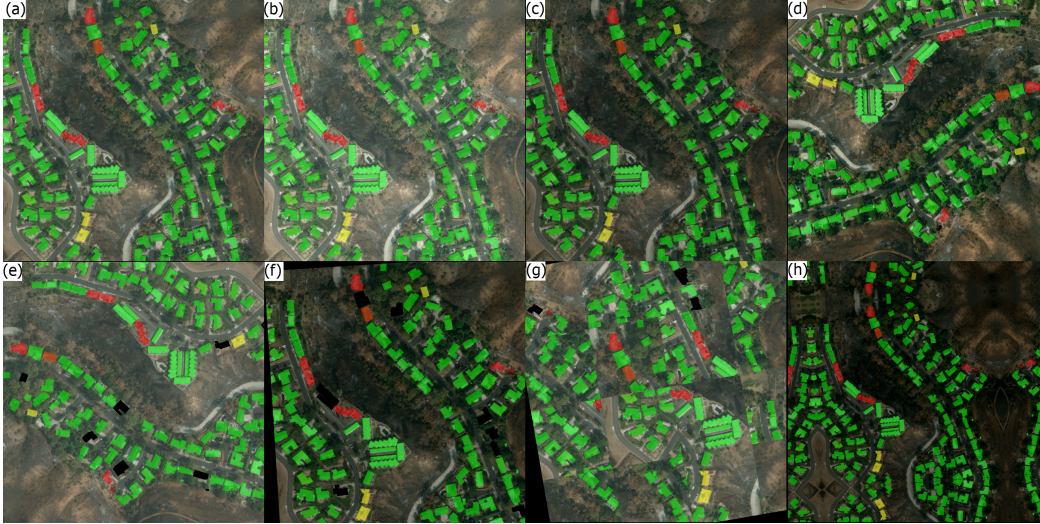


Figure 3: A satellite imagery sample with annotations (a) and its transformations (b-h).

H. Zhao, J. Shi, X. Qi, X. Wang, and J. Jia. Pyramid scene parsing network. In *2017 IEEE Conference on Computer Vision and Pattern Recognition (CVPR)*, pages 6230–6239, 2017. doi: 10.1109/CVPR.2017.660.

A Appendix A. Images augmentations

Image augmentation played a crucial part in the training pipeline. Augmentations helped prevent model overfitting, and in fact, was a critical component that increased models’ performance, especially for the pairs with significant displacement of ”pre” and ”post” images. For augmenting images, we used an open-source library Albumentations Buslaev et al. [2020] that allows creating augmented images on-the-fly during training, augments both images and corresponding masks simultaneously, and has a diverse number of supported transforms. An example of an image sample and its augmented variants is shown in Figure 3.

B Appendix B. Training procedure

Deep learning models were trained using a PyTorch framework Paszke et al. [2019] and a Catalyst library Kolesnikov [2018]. PyTorch is an efficient and flexible framework that allows the construction of custom models’ architectures and works well in this problem due to the customized input format for the models. Catalyst is a high-level framework above PyTorch that supports mixed-precision training, logging, and multi-GPUs training out of the box. For designing models’ architecture, we used a pytorch-toolbelt library Khvedchenya [2019] that allows plug-and-play change of encoders, decoders, and their parameters and provides a flexible way of creating building blocks of the model.

The training hyper-parameters for all experiments are summarized in Table 4. The batch size varied from 32 to 64 samples, depending on model architecture. We used the RAdam optimizer Liu et al. [2020] with $1e - 3$ learning rate. The full list of parameters can be found in the source code repository Khvedchenya [2020].

All models were trained on random-sized crops of 512 x 512 px size and validated on full-resolution images of 1024 x 1024 px. The best model checkpoints were chosen based on the evaluation metric. The training was performed on 4 NVidia GeForce 1080Ti GPUs and a p3.8xlarge AWS Instance, equipped with 4 NVidia Tesla V100 GPUs.

For validation, the training set was split into 5 folds. As a splitting algorithm, we used multi-label stratification based on the amount of non-damaged, minor-damaged, major-damaged, and destroyed buildings in each image and event. Such a split guarantees that each fold will contain the same distribution of damage classes with respect to event types. The alternative approach is to use a group

Table 4: Training hyper-parameters

Parameter	Description
Optimizer	RAdam
Batch size	32 .. 64
Weight decay	1e-5
Learning rate (Lr)	1e-3
Lr scheduler	Cosine decay
Minimum Lr	1e-6
Epochs	100
Train, crop size	512 x 512
Validation, image size	1024 x 1024

K-fold to ensure images from one event belong only to the same fold. Five-folds cross-validation was used to find optimal model architectures and tune hyperparameters.

C Appendix C. Ensembling

We computed the weighted average of class probabilities of all models’ predictions and then applied argmax to get class labels for each pixel in the final prediction. We computed weighting coefficients for each class by optimizing the weighted F_1 score on out-of-fold predictions. The tuned class weights for all models were [0.5, 1.1, 1.1, 1.1, 1.1], which improved weighted F_1 score at +0.01 – 0.02 for single models, and by +0.04 F_1 for the entire ensemble.

The final ensemble included 13 models from 5 folds, selected so that there were at least 2 models in the ensemble for each fold. We used different encoder backbones and Unet or FPN decoders types. The ensemble achieves a weighted F_1 score of 0.803 on the competition hold-out test.